"Characterization of a functional NTPDase in the endoplasmic reticulum of rat submandibular salivary gland"

Mariano Anibal OSTUNI.[a,b,*], Patricia EGIDO [b], Gabriel PERANZI[a], Guillermo Luis ALONSO[b], Jean-Jacques LACAPERE[a]., and Débora Alejandra GONZALEZ[b]

[a] INSERM U773, Centre de Recherche Biomédicale Bichat-Beaujon (CRB3), Université Paris 7 Denis Diderot, site Bichat . 16, rue Henri Huchard, 75870 Paris Cedex, France.

[b] Cátedra de Biofísica, Facultad de Odontología, Universidad de Buenos Aires. M.T. de Alvear 2142 C1122AAH, Buenos Aires, Argentina.

[*]Corresponding author:

Mariano A. Ostuni. INSERM U773, Centre de Recherche Biomédicale Bichat-Beaujon (CRB3). 16, rue Henri Huchard, 75870 Paris Cedex, France. Tel (+33) 1 57 27 74 80. Fax (+33) 1 57 27 74 80. E-mail address: **mariano.ostuni@inserm.fr**

Running Title: NTPDase activity in submandibular gland

Summary**.**

Nucleotidase activity and Ca-uptake were characterized in endoplasmic reticulum (ER) enriched rat submandibular gland (SMG) microsomal preparations. (i) Ca-uptake presented characteristics of an ER Ca-ATPase. (ii) Nucleotidase activity was equally stimulated by calcium, magnesium and manganese, but with different Km values. (iii) Specific inhibitors of P-type Ca-ATPases were ineffective on nucleotidase activity, demonstrating that this activity was not related to calcium uptake and did not correspond to classical Ca^{2+} pumps. (iv) ATP and UTP were more efficient substrates, whereas ADP and UDP were hydrolyzed with significantly slower rate. (v) Nucleotidase activity was sensitive to mild detergent solubilization and insensitive to ionophore addition. (vi) Nucleotidase activity was strongly inhibited by suramin, a nucleoside triphosphate diphosphohydrolase (NTPDase) inhibitor. (vii) Nucleotidase activity exponentially diminished as function of time. All these observations are consistent with a NTPDase identity. The presence of a NTPDase was demonstrated by immunohistochemistry in rat SMG. Immunoreactivity was stronger in ductal cells than in mucus and serous acini. Although this enzyme was observed in the plasma membrane, colocalization with the ER marker calnexin revealed a specific subcellular localization in this organelle of all three types of cell. The putative function of this NTPDase activity in salivary glands is discussed.

Key words: Apyrase, CD39, Ca-uptake, ATPase activity, submandibular gland.

Introduction

Submandibular glands (SMG) belong to the major salivary gland group, with important functions involved in the oral health and the digestion process. They are widely used as a model to study the secretory mechanisms in the epithelial cells.

Regulation of salivary secretion is complex and secretory agents usually act by cAMP and Ca^{2+} pathways, which could regulate the same process with opposite or synergic results.

The Ca^{2+} pathway implies the fine-tuning regulation of cytosolic calcium levels. Ca^{2+} influx from the extracellular liquid and Ca^{2+} release from intracellular calcium stores are strongly related with the cation extrusion and the stores refilling. Several pumps and calcium channels have been identified in submandibular glands. The group of S. Muallem has identified in the rat submandibular gland different calcium ATPases as the plasma membrane Ca-ATPase (PMCA) and the sarco-endoplasmic reticulum Ca-ATPase (SERCA) (Lee et al 1997a), and calcium channels like the IP3-sensitive and the ryanodyne-sensitive (Lee et al 1997b).

The functional characterization of the SERCA was usually addressed measuring the enzymatic activity and the ionic transport in submandibular endoplasmic reticulum microsomes (Alonso et al 1971; Hurley and Martínez, 1985, 1986; Hurley and Ryan 1988), but a clear correlation between Ca^{2+} uptake and ATPase activity was never well established. At present the question remains what is the actual identity of the enzymes that hydrolyze ATP in those microsomes.

Another class of ATP hydrolyzing enzymes is the family of ecto-nucleoside triphosphate diphosphohydrolases (NTDPases) that hydrolyze ATP and other nucleotides with largely higher hydrolysis rate than the Ca-ATPase pumps, but without coupled cation transport (for detailed review see Plesner 1995; Robson et al 2006). At present, eight members of this family were idientified, which are addressed to the plasma membrane and/or to intracellular membranes (Robson et al 2006).

NTPDases are ubiquitous in eukaryotic cells but their functions are not fully understood. Cumulate evidences support the involvement of these enzymes in the regulation of nucleotide concentration and adenosine recycling process. Furthermore their spatial and temporal expression in several cell types could be at the origin of different patho-physiological processes (Reviewed in Robson et al 2006).

Several articles characterizing an NTPDase like activity in the rat parotid gland were published (Dodw et al 1989, 1993, 1996, 1999; Teo et al 1993; Murphy et al 1994), but there are only a cup of papers talking about this kind of activity in rat submandibular gland (Valenzuela et al 1989, Murphy et al 1994)

In this work we characterize an ATPase activity from endoplasmic reticulum microsomes from rat submandibular gland, which has the characteristics of an ecto-nucleotidase activity and that it is not related to calcium uptake. We also identify the cellular and subcellular localization of a NTPDase immunoreactivity in this gland.

Methods

Animals

Male Wistar rats weighing 250 to 280 gr. were fed with standard chow diet and water ad libitum, and kept with 12 h light / 12 h dark period. They were treated in accordance with the European Convention for the Protection of Vertebrate Animals used for Experimental and other Scientific Purposes (CETS 123).

Microsomes preparation

Microsomes preparation protocol was modified from previously described (Hurley and Martinez 1986). Briefly, rats were allowed free access to standard chow pellets and water except for the night before sacrifice when only food was withheld. For each tissue preparation 2 to 4 rats were deeply anaesthetized by exposure to air saturated with ether and exsanguinated via the abdominal aorta. The submandibular glands were removed, separated from the adjoining sublingual glands, weighed, minced on ice and homogenized in cold buffer (10 mM HEPES, pH 7.0, 0.3 M sucrose and 1 mM of the protease inhibitor PMSF) using a teflon and glass homogenizer. The homogenate was centrifuged for 2 minutes at 1000 x g to remove nuclei and cell debris. Supernatant was centrifuged for 20 minutes at 10,000 x g, the pellet containing mitochondrial fraction was discarded and resulting supernatant was centrifuged for 30 minutes at 27,000 x g. The final pellet was re-suspended in the same buffer and proteins were quantified using the dye-binding BioRad assay.

Electron Microscopy

Microsome preparation was fixed in 2.5% glutaraldehyde during 60 min at room temperature and postfixed in 1% osmium tetroxide for 60 min. It was dehydrated and embedded in LX-112 resin and sections were contrasted with 2% uranyl acetate and observed in a JEOL 1200 EX electron microscope operated at 80 kV accelerated voltage.

Electrophoresis and Western blotting

SDS-polyacrylamide gel electrophoresis was performed according to Laemmli (Laemmli 1970). Proteins (15 µg per lane) were separated on 10 % polyacrylamide gel under non reducing conditions. They were transferred to 0.45 µm pore nitrocellulose membranes (Sartorius AG, Göttingen, Germany) and probed with monoclonal anti-hNTPDase1 antibody (BU61 clone, Ancell, Bayport, MN, USA) (1:750 dilution); or with a rabbit anti-calnexin monoclonal antibody (Becton Dickinson, Le Pont de Claix, France). (1:4000 dilution). Bands were visualized using peroxidase-conjugated anti-mouse or anti-rabbit IgG respectively (Sigma, Saint-Quentin Fallavier, France) and the Pierce ECL western blotting substrate (Thermo Scientific, Rockford, IL, USA).

Deglycosylation

Microsome preparations were subjected to deglycosylation using PNGase F (New England Biolab, Ipswich, MA, USA) following manufacturer instructions.

ATPase activity

The microsomal ATPase activity was measured at pH 7.2 and 37°C following Pi liberation. The media contained 50 mM Mops-Tris, pH 7.2, 100 mM KCl, 3 mM ATP and different amounts of $CaCl_2$ or $MgCl_2$, and EGTA to obtain the desired cation concentration. Reactions were started by addition of 0.1 mg vesicular protein per ml. After 2 min incubations the reactions were stopped by addition of cold trichloroacetic acid at 5% final concentration. Pi production was determined by a colorimetric method (Baginski et al 1967). Free cation concentrations were calculated as previously described (Fabiato and Fabiato 1979).

[^{45}Ca]Ca-uptake

Ca-uptake was measured in 1 ml of medium of the following composition: 100 mM KCl, 50 mM MOPS/Tris, pH 7.2, 3 mM ATP, 3 mM $MgCl_2$, 0.1 mM $CaCl_2$, also containing 1500 ± 500 cpm/nmol of [^{45}Ca] (New England Nuclear, Boston, MA, USA), and 0.1 mg of membrane protein. The reaction mixture lacking membrane proteins was pre-incubated for 5 min at 37 °C. Ca-uptake was started by addition of membrane proteins and aliquots of the reaction mixture were passed through Millipore filters (0.45 µm pore diameter) at the given time periods. The filters were immediately washed with 5 ml of 3 mM $LaCl_3$ in order to diminish the unspecific binding. Radioactivity was determined by liquid scintillation counting in a toluene-based scintillation cocktail.

Immunohistochemistry

Submandibular glands from 4 rats were removed and cleaned from connective tissue. They were immediately fixed in 4% paraformaldehyde during 4 hours at room temperature and embedded in paraffin. Paraffin sections were re-hydrated and endogenous peroxidase activity was inactivated followed by the peroxidase-antiperoxidase (PAP) technique. Sections were incubated with a mouse anti-human NTPDase1 (hNTPDase1) monoclonal antibody (BU61 clone, 1:100 dilution, Ancell, Bayport, MN, USA) overnight at 4°C. Peroxidase complexed secondary antibody was purchased from Dakopatts Ltd. (Trappes, France). Sections were counterstained with Mayer's hematoxilin (E.M.S.) (Euromedex, Souffelweyersheim, France).

Colocalization Studies

Paraffin sections for confocal microscopy were re-hydrated and incubated with a rabbit anti-calnexin monoclonal antibody (1:100) for 1h (Becton Dickinson, Le Pont de Claix, France). After washing, sections were incubated with a secondary anti-rabbit immunoglobulins

antibody coupled with ALEXA Fluor 488 (1:200) (Molecular Probes, Oregon, USA) and then incubated overnight at 4°C with the anti-hNTPDase1 antibody (1:100). Following second washing, secondary anti-mouse immunoglobulins antibody coupled with ALEXA Fluor 546 (Molecular Probes, Oregon, USA) was deposited for 60 min (1:150 dilution). After several washes, slides were covered with a hydrophilic and antifading mounting media (Fluoromount G, E.M.S.). Final observations were made with a Zeiss Axiovert 200M confocal microscope with a 63x oil immersion objective. LSM 510 image software (Heidelberg, Germany) was used to select observation fields (identical intensities profile of each fluorochrome), to collect the results (histograms, fluorograms, colocalizations of both dyes), and to derive data recording and analysis. Step size for the sectioning was 0.4 µm for the deconvolved images with a pinhole value fixed at 1 µm. Similar incubations without the primary antibody were also performed as negative controls.

Reagents and solutions

$C_{12}E_8$ was purchased from Calbiochem (La Jolla, CA, USA). Unless otherwise noted, all other reagents were purchased from Sigma Chemical Co. (St. Louis, MO, USA).

Statistics

Data are presented as the mean ± standard error of mean (SEM). Experimental data were studied using one-way ANOVA. Scheffe homogeneity test was performed in order to determinate differences between means of each experimental group and control counterpart. Differences were considered significant for $p< 0.05$.

Results

Electron Microscopy and western blot.

Figure 1a shows typical image of section from microsomal preparation included in resin. Vesicles surrounded by large dots corresponding to ribosomes are clearly observed and characteristics of rough ER microsomes. Dotted surfaces are also observed and correspond to surfaces of vesicles that have not been sectioned. It has to be mentioned that neither mitochondria nor mitochondrial fragments were observed in these microsomal preparations. The ER origin of these microsomes was confirmed by western blot with the presence of a characteristic band of 88 kDa that corresponds to the ER specific protein calnexin, (Fig. 1b).

[^{45}Ca]Ca-Uptake.

Figures 1c and 1d show time dependent Ca-uptake from SMG microsomes. Panel c demonstrates ATP dependence of this uptake, resulting in an increase of calcium inside the vesicles, observed only in the presence of ATP. A fast release of Ca^{2+} was triggered by addition of Ca^{2+} ionophore A23187..

The effect of two SERCA inhibitors on Ca-uptake are shown in the Fig 1d. Thapsigargin and sodium orthovanadate diminished the Ca^{2+} uptake from SMG microsomes by about 90 %. The mitochondrial Ca-uniporter inhibitor ruthenium red and the PMCA inhibitor compound 48/80 had no effect on SMG microsomes Ca^{2+} uptake (data not shown). These are the first results about the ATPase inhibitors action on the rat submandibular Ca^{2+} uptake. They confirm the microsomal origin of the ER membranes while minimizing the possibility of mitochondrial or plasma membrane contamination.

ATPase Activity

To functionally characterize the ATPase activity in our micromal preparation, we tested: i) the dependence on Ca^{2+} and/or Mg^{2+}, (ii) the sensitivity to specific inhibitors of P-type, F-type, and V-type ATPases, (iii) the substrate preference pattern, (iv) the sensitivity to the action of detergents and (v) the dependence on incubation time.

Figure 2a shows ATPase activity of SMG microsomes as function of free Mg^{2+} with no added calcium or free Ca^{2+} without added magnesium. Maximal activities were similar for both conditions (around 1 µmol Pi produced/mg protein/min) but the Km values calculated from plots were different with values of 28 ± 5 µM and 320 ± 51 µM for Ca^{2+} and Mg^{2+}, respectively. ATPase activity was also stimulated by Mn^{2+} (open squares). Maximal activity was reached in the presence of mM concentration of Ca^{2+} or Mg^{2+} irrespective of other cation concentration (data not shown).

Table 1 shows the effect of different ATPase inhibitors. No significant inhibition of ATPase activity was obtained by the SERCA inhibitor thapsigargin, the P-type ATPases inhibitor sodium orthovanadate, the PMCA inhibitor compound 48/80, or the Na/K ATPase inhibitor ouabain. However, sodium azide, an unspecific NTPDase inhibitor (Knowles and Nagy 1999; Schetinger et al 2001), slightly diminishes ATPase activity (67.4 % of control), while suramin, a NTPDase inhibitor (Iqbal et al 2005), produces a strong inhibition of this activity. Figure 2b showed the concentration-dependent inhibition profile from which IC_{50} could be calculated giving values of 55 ± 10 µM and 585 ± 160 µM for suramin and sodium azide, respectively. The simultaneous addition of suramin and sodium orthovanadate at saturating concentrations produced an additional 5 % inhibition, whereas addition of calcium ionophore A23187 did not change ATPase activity.

Hydrolysis of different tri- and di- nucleotides are presented in figure 2c. The SMG microsomes nucleotidase activity is principally a tri-nucleotidase activity. ATP and UTP are largely hydrolyzed compared to ADP or UDP. ATP/ADP and UTP/UDP hydrolysis ratio are 4.39 and 4.93, respectively. Figure 2d shows that ATPase activity decayed exponentially. Differential activity values were obtained from the derivative of the Pi production as function of time (not shown)

These results strongly suggest that this ATPase activity resulted from an NTPDase. Moreover, addition of detergent $C_{12}E_8$ significantly inhibited the ATPase activity of SMG microsomes (28 % of control, table 1). If this ATPase activity was the product of a SERCA type enzyme, mild detergent solubilization would augment activity by abolishing inhibition by intravesicular Ca^{2+} concentration. Furthermore, it has been previously described that detergent had a strong inhibitory effect on NTPDase activity (Wang and Guidotti 1998).

Cation and substrate specificity, inhibitors effect, and detergent sensitivity, indicate the presence of one or several NTPDases, probably belonging to the NTPDase1 related enzymes (NTPDases 1, 2, 3 and 8), which are usually located in the plasma membrane. However different articles reported NTPDase1 activity in subcellular compartments in eukaryotic cells (Zhong et al 2001; D'Alessio et al 2003) opening the question about the possible intracellular function of these enzymes.

Immunohistochemistry:

Based on the highly conserved amino acid sequence of different NTPDases among species, we tested the specificity of a commercially available anti human NTPDase1 (hNTPDase1) monoclonal antibody.

Western blot performed from non reducing conditions PAGE revealed that this antibody was able to recognize a band of 78 kDa both in human platelets lysate as well as in rat whole homogenate and microsomal fraction (Fig. 3a, lanes 1-3). It's noteworthy that 54 kDa bands are proportionally most important in SMG microsomal fraction compared to SMG whole homogenate, indicating that microsomal fraction presented a significant amount of non glycosylated enzyme (Lemmens et al 2000). After PNGase F digestion, microsomal fraction showed a reduced 78 kDa band and the presence of a new band of about 28 kDa (Fig 3 lane 4).

Figure 3b-e shows rat SMG immunoreactivity against anti-hNTPDase1 monoclonal antibody. As expected, immunoreactivity was strongly revealed in blood vessels, which are well known to express high levels of NTPDases. Cells of epithelial ducts (Figs. 3b,c) and mucous acini (Figs. 3b,d) are homogeneously labelled, whereas only 20% of serous acini were anti hNTPDase1 positive (Figs. 3b,e). Figures 3c-e reveal that immunoreactivity was located both in the plasma membrane and in the cytosol of rat SMG cells with stronger reactivity in the plasma membrane of luminal pole (Figs. 1c-e, arrows heads). NTPDase immunoreactivity was principally located in the luminal pool of duct cells, whereas labeling in serous and mucous acini is distributed through the cells. This difference might be accounted by the nuclear localization of duct cells near the luminal membrane, while acinar cells nuclei are distributed throughout the cytoplasm.

Distribution of NTPDase immunoreactivity presented herein was different to one described in the mouse SMG where mucous acini were weakly stained while duct cells were not reactive to anti CD39 polyclonal antibody at all (Kittel et al 2004).

Immunofluorescence and colocalization

Present observations of NTPDase1-like immunoreactivity in the cytosol (Fig. 3c-e) suggest localization in the endoplasmic reticulum. This hypothesis was tested by immunofluorescence colocalization experiments using two antibodies reacting to NTPDase1 and to calnexin (specific endoplasmic reticulum protein (Bergeron et al. 1994)). In figure 4 anti calnexin immunoreactivity (a,d,g), anti NTPDase1 labeling (b,e,h) and colocalization images (c,f,i) from duct cells (a,b,c), mucous acini (d,e,f) and serous acini (g,h,i) are respectively shown. The three cell types show positive anti-NTPDase immunofluorescence (red) and a strong reaction to anti-calnexin antibodies (green). Anti-calnexin immunoreactivity presents the typical perinuclear pattern of ER localization.

Colocalization analysis was made using the same fluorescence intensity for both signals and pixel-to-pixel superposition was only considered as a valid colocalization point. Figure 4

(c,f,i) shows that NTPDase1 immunoreactivity strongly colocalized with calnexine both in duct cells (c), mucous acinar cells (f) and serous acinar cells (i).

Discussion

We studied active Ca^{2+} transport and ATPase activity in rat submandibular gland using an endoplasmic reticulum enriched microsomes preparation (Hurley and Martinez 1986). Ca^{2+}-uptake by the microsomes was completely abolished by P-type ATPases or SERCA inhibitors. These results give the first information about specific inhibitor actions on submandibular Ca^{2+} uptake, and agree with the presence of a SERCA pump in submandibular gland (Lee et al 1997a). However, both rate and maximal amount of accumulated Ca^{2+} were lower than those measured in the well-known sarcoplasmic reticulum (SR) from rabbit skeletal muscle (Gonzalez et al 2003). Since SR contains only the SERCA1 isoform, this difference might result from the expression of SERCA isoforms SERCA3 and SERCA2 in the SMG (Lee et al 1997a). It is also possible that this difference might be the result of a minor SERCA concentration in microsomes from SMG.

High sensitivity to thapsigargin discards the possibility of a secretory pathway calcium ATPase (SPCA) since, the pumps involved in this process are thapsigargin insensitive (Van Baelen et al 2004; Vanoevelen et al 2005).

The mean of the work was to determine whether the ATPase activity measured in the microsomes is only a result of a SERCA activity. In skeletal muscle, addition of calcium ionophore A23187 to impermeable vesicles enriched in SERCA enhances the ATPase activity since it prevents calcium accumulation and consequent ATPase inhibition (Gonzalez et al 2006). Same effect is usually found by addition of mild detergents, which produces total or partial enzyme solubilization. However, ATPase activity in our vesicles was not modified by ionophore addition, and it was strongly inhibited in the presence of $C_{12}E_8$. Furthermore, activity was significantly inhibited by sodium azide and by suramin, two drugs that are effective to inhibit NTPDases (Knowles and Nagy 1999; Schetinger et al 2001; Failer et al 2003; Iqbal et al 2005). Simultaneous addition of saturating concentrations of suramin and sodium orthovanadate revealed additive effects, supporting the hypothesis of at least two different ATP-hydrolyzing enzymes in the microsomal preparation.

When characterizing cation dependence of ATPase activity we found that, although having more affinity for calcium, it could be also activated by magnesium or manganese when calcium was absent as described for NTPDases (Mihaylova-Ttodorova Svletana et al 2002) and SPCA (Van Baelen et al 2004), respectively. Km values for these cations were significantly slower than described Km values in SERCA (Gonzalez et al 2006) or SPCA (Van Baelen et al 2004; Vanoevelen et al 2005), but similar to those reported for NTPDases (Mihaylova-Ttodorova Svletana et al 2002). The manganese activation was previously

described for different plasma membrane Mg-ATPase (Beeler et al 1985; Zhao and Dhalla 1988) but in those reports activation rates were even lower for Mn compared to Mg. Conversely, results presented herein showed similar activation rates for both cations in accordance with recent data obtained with a *Trypanosoma Brucei* NTPDase (de Souza Leite et al 2007) .

Microsomes nucleotidase activity had a wide range of substrate specificity, presenting significantly higher hydrolysis rate for nucleotide tri phosphates (ATP and UTP) than for nucleotide diphosphates (ADP and UDP). Finally, ATPase activity decayed as a function of time, as was previously described for Ca-independent Mg-ATPases (Beeler et al 1995), the Ca/Mg ATPase of rat heart plasma membrane (Zhao and Dhalla 1988) or, more specifically, for human NTPDase2 (Knowles and Chiang 2003).

All these results support the hypothesis that the endoplasmic reticulum microsomes from rat submandibular gland express at least two different enzymes responsible for calcium uptake and nucleotidase activity. The biochemical characteristics of nucleotidase activity agree with an ecto-nucleoside triphosphate diphosphohydrolase (E-NTPDase) activity (Plesner 1995; Heine et al 1999; Iqbal et al 2005; Kukulski et al 2005).

Eight members of E-NTPDase family have been characterized up to date in several tissues. They hydrolyze nucleoside triphosphates and diphosphates with wide affinity range for different substrates (Zimmermann 2001; Wu et al 2005; Kukulski et al 2005). NTPDase1 (CD39), NTPDase2 (CD39L1), NTPDase3 (CD39L3) and NTPDase8 are typical ecto-enzymes localized in the plasma membrane (Reviewed in Grinthal and Guidotti 2006), and they could be grouped as NTPDase1 related enzymes. NTPDase1 is the prototype member of this group and it has been described as a detergent-sensitive dimeric active form (Wang et al 1998) that is usually located in the plasma membrane but that can be also expressed in different cytoplasmic compartments in yeast and mammals (Zhong et al 2001; D'Alesio et al 2001; Wang et al 2005. The other four members of this enzyme family (NTPDase4-7) have a specific intracellular localization (Wang and Guidotti 1998; Mulero et al 1999; Briederbick et al 2000).

The presence of a NTPDase in three cellular types of the rat submandibular gland was described using an anti-hNTPDase1 antibody (Fig. 3b-e). This antibody was able to recognize two bands from rat submandibular gland homogenates or microsome preparation (Fig. 3a, lanes 2-3) and was demonstrated to cross react with human platelets (Fig. 3a, lane 1). Moreover, after deglycosylation, microsome preparation presented a third band corresponding to deglycosylated form (Fig. 3a, lane 4). Immunohistochemistry revealed a strong

immunoreactivity at the plasma membrane of blood vessels as well as acinar and duct cells. However, there was also important cytosolic anti-NTPDase1 immunoreactivity in salivary cells. Since cytosolic NTPDase localization well correlated with the specific ER marker calnexin (Figs. 4), it could be speculated that NTPDase described herein is one of the four intracellular members of the NTPDase family (NTPDase4-7). The two splicing variants of NTPDase4 (LALP70) hydrolyze a variety of nucleoside tri- and diphosphates and show insignificant catalytic activity towards ATP or ADP as substrates (Wang and Guidotti 1998; Biederbick et al 2000). ER- and Golgi-allocated NTPDase5 (CD39L4) and NTPDase6 (CD39L2) preferentially hydrolyze nucleoside diphosphate (Trombetta & Helenius 1999; Mulero et al 1999; Braun et al, 2000). Finally, NTPDase7 (LALP1) has an intracellular membranes distribution and hydrolyzes a variety of nucleoside tri- and diphosphates with a higher preference for UTP than for ATP (Shi et al 2001). The substrate specificity of nucleotidase activity measured in submandibular gland microsomes (Figure 2c) excludes the hypothesis that main activity was the product of any of these intracellular isoforms. The other members of NTPDase family are usually found in the plasma membrane. However, Zhong et al. demonstrated that, when transfected with a CD39-like apyrase, Cos7 cells presented this enzyme in the endoplasmic reticulum (Zhong et al 2001). It should be taking into account that maturation process of several plasma membrane proteins occurs in the ER. These authors showed an incomplete glycosylation pattern and a reduced activity (Zhong et al 2001). Present results support the hypothesis that this may be the case in ER enriched fractions from rat SMG. Indeed, (i) the NTPDase activity of SMG microsomal ER-enriched fraction was ten fold lower than recently reported NTPDase activity from rat SMG acinar cells (Henz et al 2006) and (ii) we show the presence of a 54 kDa band corresponding to a deglycosylated form of the enzyme in the ER, compared with the 78 kDa band (glycosylated protein) which is the most abundant form in the SMG whole homogenate (Fig. 3a, lanes 2-4). Suramin inhibition pattern and substrate specificity could indicate the presence of an NTPDase2 or NTPDase3 (Kukulski et al 2005; Iqbal et al 2005), however, biochemical characterization of NTPDase activity is not enough to distinguish among NTPDases 1, 2, 3 or 8.

The question about the putative function of this NTPDase in the ER of SMG remains open since, on one hand, it was proposed that high nucleotidase activity in the intracellular compartments could deplete ATP and potentially inhibits other ATP-dependent components and processes (Braakman et al 1992), but on the other hand, the presence of an active intracellular NTPDase activity was associated with several secretory processes. It was found in secreted vesicles observed in the lumen of pancreatic acini (Beaudoin et al 1986) as well as

in the pancreatic juice (Yegutkin et al 2006), the oviduct (Rosenberg et al 1977; Knowles and Nagy 1999) and the prostatic fluid (Ronquist and Brody 1985). NTPDases could play an important role in vesicle trafficking and protein glycosylation (Trombetta and Helenius 1999; Beaudoin et al 1986) by modifying substrate concentrations regulating activities of enzymes involved in these processes. This hypothesis supports NTPDase distribution in SMG, where ductal and mucus acinar cells are directly involved in the secretory process of highly glycosylated mucins. Another non exclusive hypothesis is that functional NTPDases from submandibular ER might play an active role in regulating ATP concentration in duct saliva. It was recently demonstrated that ATP is secreted by pancreatic acinar cells and that ATP concentration is modified during its passage through the ductal system by the action of NTPDase-like enzymes secreted to ductal lumen (Yegutkin et al 2006). Luminal ATP concentration is crucial to control calcium signal triggered by purinergic receptor (P2R). Indeed, it was demonstrated both in pancreatic and salivary acinar and duct cells, that expression and sensitive of P2R were heterogenic (Lee et al 1997c, Li et al 2003, Yegutkin et al 2006), with predominant expression of ATP/UTP sensitive receptors than ADP/UDP sensitive receptors in duct cells.

Our results demonstrated that both, SERCA and NTPDase like enzymes are present in submandibular gland ER. The former is responsible to calcium uptake restoring cytosolic calcium to baseline levels before stimulation. The later could be involved in the control of ductal ATP concentration which, in turns, would modulate purinergic signaling cascade.

Acknowledgements

This work was supported by the Institut National de la Santé et de la Recherche Médicale (INSERM), the Centre National de la Recherche Scientifique (CNRS), and grants from the Universidad de Buenos Aires (OD027) and the CONICET from Argentina (PIP02503). M.A. Ostuni was the recipient of doctoral fellowship from the Universidad de Buenos Aires and a postdoctoral fellow from the INSERM. The authors are grateful to Dr. B. Vidic for helpful discussions and careful reading of the manuscript, Dr. E. Ogier-Denis for kindly providing anti-Calnexin antibody, and Dr. M. Jandrot-Perrus for kindly providing human platelets lysate.

References

ALONSO GL, BAZERQUE PM, ARRIGO DM, TUMILASCI OR: Adenosine triphosphate--dependent calcium uptake by rat submaxillary gland microsomes. *J Gen Physiol* **58**: 340-350, 1971.

BAGINSKI ES, FOA PP, ZAK B: Microdetermination of inorganic phosphate, phospholipids, and total phosphate in biologic materials. *Clin Chem* **13**: 326-332, 1967.

BEAUDOIN AR, VACHEREAU A, GRONDIN G, ST JEAN P, ROSENBERG MD, STROBEL R: Microvesicular secretion, a mode of cell secretion associated with the presence of an ATP-diphosphohydrolase. *FEBS Lett* **203**: 1-2, 1986.

BEELER TJ, WANG T, GABLE K, LEE S: Comparison of the rat microsomal Mg-ATPase of various tissues. *Arch Biochem Biophys* 243: 644-654, 1985.

BERGERON JJ, BRENNER MB, THOMAS DY, WILLIAMS DB: Calnexin: a membrane-bound chaperone of the endoplasmic reticulum. *Trends Biochem Sci* **19**: 124-128, 1994.

BIEDERBICK A, KOSAN C, KUNZ J, ELSASSER HP: First apyrase splice variants have different enzymatic properties. *J Biol Chem* **275**: 19018-19024, 2000.

BRAAKMAN I, HELENIUS J, HELENIUS A: Role of ATP and disulphide bonds during protein folding in the endoplasmic reticulum. *Nature* **356**: 260-262, 1992.

BRAUN N, FENGLER S, EBELING C, SERVOS J, ZIMMERMANN H: Sequencing, functional expression and characterization of rat NTPDase6, a nucleoside diphosphatase and novel member of the ecto-nucleoside triphosphate diphosphohydrolase family. *Biochem J* **351**: 639-647, 2000.

D'ALESSIO C, TROMBETTA ES, PARODI AJ: Nucleoside diphosphatase and glycosyltransferase activities can localize to different subcellular compartments in Schizosaccharomyces pombe. *J Biol Chem* **278**: 22379-22387, 2003.

DE SOUZA LEITE M, THOMAZ R, FONSECA FV, PANIZZUTTI R, VERCESI AE, MEYER-FERNANDES JR: Trypanosoma brucei brucei: biochemical characterization of ecto-nucleoside triphosphate diphosphohydrolase activities. *Exp Parasitol* **115**: 315-323, 2006.

DOWD FJ, PASIENIUK JA, HAND AR, CHEUNG PH, HAINES DW: Characteristics of anion-stimulated Mg-ATPase from rat parotid gland secretory granules. *Arch Oral Biol* **34**: 167-176, 1989.

DOWD FJ, LI LS, CAMPBELL JE, CHEUNG PH: Localization and characterization of a parotid Ca(2+)-dependent ecto-ATPase. *Crit Rev Oral Biol Med* **4**: 415-419, 1993.

DOWD FJ, MURPHY HC, LI L: Metabolism of extracellular ATP by rat parotid cells. *Arch Oral Bio*; **41**: 855-862, 1996

DOWD FJ, LI LS, ZENG W: Inhibition of rat parotid ecto-ATPase activity. *Arch Oral Biol* **44**: 1055-1062, 1999.

FABIATO A, FABIATO F: Calculator programs for computing the composition of the solutions containing multiple metals and ligands used for experiments in skinned muscle cells. *J Physiol (Paris)* **75**: 463-505, 1979.

FAILER BU, ASCHRAFI A, SCHMALZING G, ZIMMERMANN H: Determination of native oligomeric state and substrate specificity of rat NTPDase1 and NTPDase2 after heterologous expression in Xenopus oocytes. *Eur J Biochem* **270**: 1802-1809, 2003.

GONZALEZ DA, OSTUNI MA, LACAPERE JJ, ALONSO GL: A model accounting for the simultaneous transport of calcium and manganese in sarcoplasmic reticulum membranes. *Ann N Y Acad Sci* **986**: 320-322, 2003.

GONZALEZ DA, OSTUNI MA, LACAPERE JJ, ALONSO GL: Stoichiometry of ATP and metal cofactor interaction with the sarcoplasmic reticulum Ca(2+)-ATPase: a binding model accounting for radioisotopic and fluorescence results. *Biophys Chem* **124**: 27-34, 2006.

GRINTHAL A, GUIDOTTI, G: CD39, NTPDase 1, is attached to the plasma membrane by two transmembrane domains. Why? *Purinergic. Signal.* **2**: 391-398, 2006.

HENZ SL, RIBEIRO CG, ROSA A, CHIARELLI RA, CASIALI EA, SARKIS JJ: Kinetic characterization of ATP diphosphohydrolase and 5'-nucleotidase activities in cells cultured from submandibular salivary glands of rats. *Cell Biol Int* **30**: 214-220, 2006.

HURLEY TW, RYAN MP. The control of cytosolic Ca2+ concentration: studies of high affinity Ca2+ transport in permeabilized acini of rat submandibular glands. *Arch Oral Biol* **33**: 793-800, 1988.

HURLEY TW, MARTINEZ JR: Characterization of the kinetic and regulatory properties of high-affinity Ca2+-ATPase activity in acinar preparations of rat submandibular salivary glands. *Arch Oral Biol* **30**: 587-594, 1985.

HURLEY TW, MARTINEZ JR: Characterization and localization of two forms of active Ca2+ transport in vesicles derived from rat submandibular glands. *Cell Calcium* **7**: 49-59, 1986.

IQBAL J, VOLLMAYER P, BRAUN N, ZIMMERMANN H, MULLER CE: A capillary electrophoresis method for the characterization of ecto-nucleoside triphosphate diphosphohydrolases (NTPDases) and the analysis of inhibitors by in-capillary enzymatic microreaction. *Purinergic. Signal.* **1**: 349-358, 2005.

KITTEL A, PELLETIER J, BIGONNESSE F, GUCKELBERGER O, KORDAS K, BRAUN N, ROBSON SC, SEVIGNY J: Localization of nucleoside triphosphate diphosphohydrolase-1 (NTPDase1) and NTPDase2 in pancreas and salivary gland. *J Histochem Cytochem* **52**: 861-871, 2004.

KNOWLES AF, NAGY AK: Inhibition of an ecto-ATP-diphosphohydrolase by azide. *Eur. J. Biochem.* **262**: 349-357, 1999.

KNOWLES AF, CHIANG W-C: enzymatic and transcriptional regulation of human ecto-ATPase/E-NTPDase 2. *Arch Biochem Biophys* 418: 217-227, 2003.

KUKULSKI F, LEVESQUE SA, LAVOIE EG, LECKA J, BIGONNESSE F, KNOWLES AF, ROBSON SC, KIRLEY TL, SEVIGNY J: Comparative hydrolysis of P2 receptor agonists by NTPDases 1, 2, 3 and 8. *Purinergic. Signal.* **1**: 193-204, 2005.

LAEMMLI UK: Cleavage of structural proteins during the assembly of the head of bacteriophage T4. *Nature* **227**: 680-685, 1970.

LEE MG, XU X, ZENG W, DIAZ J, KUO TH, WUYTACK F, RACYMAEKERS L, MUALLEM S: Polarized expression of Ca2+ pumps in pancreatic and salivary gland cells. Role in initiation and propagation of [Ca2+]i waves. *J Biol Chem* **272**: 15771-15776, 1997a.

LEE MG, XU X, ZENG W, DIAZ J, WOJCIKIEWICZ RJ, KUO TH, WUYTACK F, RACYMAEKERS L, MUALLEM S: Polarized expression of Ca2+ channels in pancreatic and salivary gland cells. Correlation with initiation and propagation of [Ca2+]i waves. *J. Biol. Chem.* **272**: 15765-15770, 1997b.

LEE MG, ZENG W, MUALLEM S: Characterization and localization of P2 receptors in rat submandibular gland acinar and duct cells. *J Biol Chem.* **272**: 32951-3295, 1997c.

LEMMENS R, KUPERS L, SEVIGNY J, BEAUDOIN AR, GRONDIN G, KITTEL A, WAELKENS E, VANDUFFEL L: Purification, characterization, and localization of an ATP diphosphohydrolase in porcine kidney. *Am J Physiol Renal Physiol* **278**: F978-F988, 2000.

LI Q, LUO X, ZENG W, MUALLEM S: Cell-specific behavior of P2X7 receptors in mouse parotid acinar and duct cells. *J Biol Chem.* **278**: 47554-47561, 2003.

MIHAYLOVA-TODOROVA ST, TODOROV LD, WESTFALL DP: Enzyme kinetics and pharmacological characterization of nucleotidases releasedfrom the guinea pig isolated vas deferens during nerve stimulation: evidence for a soluble ecto-nucleoside triphosphate diphosphohydrolase-like ATPase and a soluble ecto-5'-nucleotidase-like AMPase. *J Pharmacol Exp Ther* **302**: 992-1001, 2002.

MULERO JJ, YEUNG G, NELKEN ST, FORD JE: CD39-L4 is a secreted human apyrase, specific for the hydrolysis of nucleoside diphosphates. *J Biol Che*; **274**: 20064-20067, 1999.
MURPHY HC, HAND AR, DOWD FJ: Localization of an ecto-ATPase/cell-CAM 105 (C-CAM) in the rat parotid and submandibular glands. *J Histochem Cytochem* **42**: 561-568, 1994.
PLESNER L: Ecto-ATPases: identities and functions. *Int Rev Cytol* **158**: 141-214,1995.
ROBSON SC, SEVIGNY J, ZIMMERMANN H: The E-NTPDase family of ectonucleotidases: Structure function relationships and pathophysiological significance. *Purinergic. Signal.* **2**: 409-430, 2006.
RONQUIST G, BRODY I: The prostasome: its secretion and function in man. *Biochim Biophys Acta* **822**: 203-218, 1985.
ROSENBERG MD, GUSOVSKY T, CUTLER B, BERLINER AF, ANDERSON B: Purification and characterization of an extracellular ATPase from oviductal secretions. *Biochim Biophys Acta* **482**: 197-212, 1977.
SCHETINGER MR, VIEIRA VL, MORSCH VM, BALZ D: ATP and ADP hydrolysis in fish, chicken and rat synaptosomes. *Comp Biochem. Physiol B Biochem. Mol. Biol.* **128**: 731-741, 2001.
SHI JD, KUKAR T, WANG CY, LI QZ, CRUZ PE, DAVOODI-SEMIROMI A, YANG P, GU Y, LIAN W, WU DH, SHE JX: Molecular cloning and characterization of a novel mammalian endo-apyrase (LALP1). *J Biol Chem* **276**: 17474-17478, 2001.
TEO TS, THIYAGARAJAH P, LEE MK, SELWYN MJ: The high-affinity Ca(2+)-ATPase from rat parotid plasma membranes is an ectoenzyme: solubilization and characterization of the Ca(2+)-ATPase activity. *Biochem Med Metab Bio*; **50**: 358-362, 1993.
TROMBETTA ES and HELENIUS A: Glycoprotein reglucosylation and nucleotide sugar utilization in the secretory pathway: identification of a nucleoside diphosphatase in the endoplasmic reticulum. *EMBO J* **18**: 3282-3292, 1999.
VALENZUELA MA, LOPEZ J, DEPIX M, MANCILLA M, KETTLUN AM, CATALAN L, CHIONG M, GARRIDO J, TRAVERSO-CORI A: Comparative subcellular distribution of apyrase from animal and plant sources. Characterization of microsomal apyrase. *Comp Biochem Physiol B* **93**: 911-919, 1989.
VAN BAELEN K, DODE L, VANOEVELEN J, CALLEWAERT G, DE SMEDT H, MISSIAEN L, PARYS JB, RAEYMAEKERS L, WUYTACK F: The Ca2+/Mn2+ pumps in the Golgi apparatus. *Biochim Biophys Acta* **1742**: 103-112, 2004.

VANOEVELEN J, DODE L, VAN BAELEN K, FAIRCLOUGH RJ, MISSIAEN L, RAEYMAEKERS L, WUYTACK F: The secretory pathway Ca2+/Mn2+-ATPase 2 is a Golgi-localized pump with high affinity for Ca2+ ions. *J Biol Chem* **280**: 22800-22808, 2005.
WANG CJ, VLAJKOVIC SM, HOUSLEY GD, BRAUN N, ZIMMERMANN H, ROBSON SC, SEVIGNY J, SOELLER C, THORNE PR: C-terminal splicing of NTPDase2 provides distinctive catalytic properties, cellular distribution and enzyme regulation. *Biochem J* **385**: 729-736, 2005.
WANG TF, GUIDOTTI G: Golgi localization and functional expression of human uridine diphosphatase. *J Biol Chem* **273**: 11392-11399, 1998.
WANG TF, OU Y, GUIDOTTI G: The transmembrane domains of ectoapyrase (CD39) affect its enzymatic activity and quaternary structure. *J Biol Chem* **273**: 24814-24821, 1998.
WU JJ, CHOI LE, GUIDOTTI G: N-linked oligosaccharides affect the enzymatic activity of CD39: diverse interactions between seven N-linked glycosylation sites. *Mol Biol Cell* **16**: 1661-1672, 2005.
YEGUTKIN GG, SAMBURSKI SS, JALKANEN S, NOVAK I: ATP-consuming and ATP-generating enzymes secreted by pancreas. *J Biol Chem.* **281**: 29441-29447, 2006.
ZHAO D, DHALLA NS: Characterization of rat heart plasma membrane Ca2+/Mg2+ ATPase. *Arch Biochem Biophys* 263: 281-292, 1988.
ZHONG X, MALHOTRA R, WOODRUFF R, GUIDOTTI G: Mammalian plasma membrane ecto-nucleoside triphosphate diphosphohydrolase 1, CD39, is not active intracellularly. The N-glycosylation state of CD39 correlates with surface activity and localization. *J Biol Chem* **276**: 41518-41525, 2001.
ZIMMERMANN H. Purinergic and Pyrimidergic Signalling I. In Abbracciio MP and Williams M (ed). *Handbook of Experimental Pharmacology*. Srpinger Verlag, Heidelber 209-250, 2001.

Table 1. Effects of inhibitors on ATP hydrolysis by rat submandibular microsomes.

Inhibitor	ATPase Activity (% of Control)
Thapsigargin (2 µM)	89.7 ± 12.6
Sodium orthovanadate (1 mM)	89.8 ± 7.8
Ouabain (0.1 mM)	95.5 ± 10.5
Compound 48/80 (1 mg/ml)	89.3 ± 9.3
Sodium azide (10 mM)	67.4 ± 11.5*
Suramin (3 mM)	19.7 ± 2.0**
Suramin (3 mM) + sodium orthovanadate (1mM)	13.4 ± 2.9**
$C_{12}E_8$ (detergent/protein = 3 w/w)	28.0 ± 2.0**
Ionophore (A23187 5 µM)	98.0 ± 4.5

Control ATPase activity (100%) was 1.24 ± 0.09 µmol Pi/mg protein/min. Results are expressed as mean ± S.E.M. (n = 5). Data were analyzed statistically by one-way analysis of variance (ANOVA). * $p < 0.05$ ** $p < 0.01$

Figure Legends

Figure 1: ER origin and calcium uptake by rat submandibular microsomes (a) Electron micrograph of a thin section of the microsome preparation showed typical rough microsomes (arrows indicated the ribosomes bound to the vesicles, bar = 200 nm). (b) Western blot for identification of Calnexin. Immunoreactivity of microsomes from rat submandibular endoplasmic reticulum with a rabbit anti-calnexin monoclonal antibody. (c) Calcium uptake was measured at 37 °C, pH 7.2, 50 µM $^{45}Ca(CaCl_2)$, 100 mM KCl, 3 mM $MgCl_2$, with (triangles) or without (circles) 3 mM ATP. As indicated by arrow, 5µM calcium ionophore A23187 was added. (d) Experiments were made with identical control condition (triangles) but in the presence of 1 mM sodium orthovanadate (squares) or 2 µM thapsigargin (circles). Each point is a result of at least 5 independent experiments. Results are expressed as mean ± S.E.M.

Figure 2: ATPase activity in rat submandibular microsomes. Cation dependence, inhibitor's action, substrate specificity and time dependence (a) ATPase activity was plotted as function of $[Ca^{2+}]$ (triangles) without added Mg, or as function of $[Mg^{2+}]$ (filled squares) or $[Mn^{2+}]$ (open squares), without added Ca. Experiments were made at 37 ºC with 3 mM ATP. Inset: Linewever-Burk double reciprocal plots. (b) Effect of suramin (circles, IC_{50} = 55 ± 10 µM) and sodium azide (triangles, IC_{50} = 585 ± 160 µM) on nucleotidase activity. (c) Substrate specificity of nucleotidase activity. Control ATPase activity (100%) was 1.24 ± 0.09 µmol/mg protein/min. All substrates were used at 3 mM (0.1 mM Ca^{2+}). (d) ATPase activities were calculated as dPi/dt values from the derivative of the curve obtained for Pi as a function of time. Each point is a result of at least 5 independent experiments. Results are expressed as mean ± S.E.M. * $P < 0.05$; *** $P<0.001$

Figure 3: CD39 immunostaining in rat submandibular gland. Panel a: cross-reactivity of anti hNTPDase1 monoclonal antibody was revealed by Western Blot showing positive reactivity with human platelet lysate (lane 1), rat SMG whole homogenate (lane 2), rat SMG microsomes (lane 3) and rat SMG microsomes after deglycosylation by PNGase (lane 4). Panel b: Brown color of peroxydase-antiperoxydase (PAP) revealed the anti-hNTPDase1 immunoreactive cells in rat SMG counterstained with haematoxylin. Immunoreactivity is present in blood vessels (bv), secretory ducts (du) and mucous acini (ma) but only in some serous acini (sa). Panels c, d and e show cellular localization with a higher magnification,

arrow heads indicates plasma membrane strong immunoreactivity. All duct cells were immunoreactive, with apical area strongly labeled (c). Depleted mucous cells (d) and acinar serous cells (e) were uniformly stained. Bars: (b) = 100 µm, (c, d, and e) = 10 µm. L = lumen

Figure 4: CD39 and calnexin colocalization by confocal microscopy immunofluorescence. Calnexin immunostaining was revealed by an anti-calnexin Ab coupled to Alexa Fluor 488 (green a, d, g) and that of CD39 by an anti-CD39 monoclonal Ab coupled to Alexa 546 (red b, e, h). Cytoplasmic Anti calnexin immunoreactivity was found in duct cells (a), mucous acinar cells (d) and serous acinar cells (g). Duct (b), mucous (e) and serous (h) cells were anti CD39 immunostained. White points in figures c, f, and i indicate that both proteins colocalize at a narrow perinuclear area. L = lumen N = nucleus, SG = secretory granules. Bar = 5 µm.

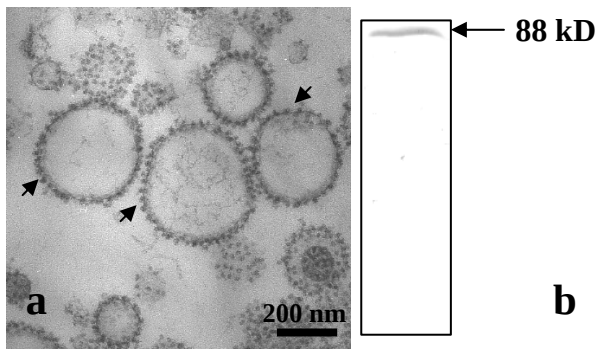
88 kD
a
200 nm
b

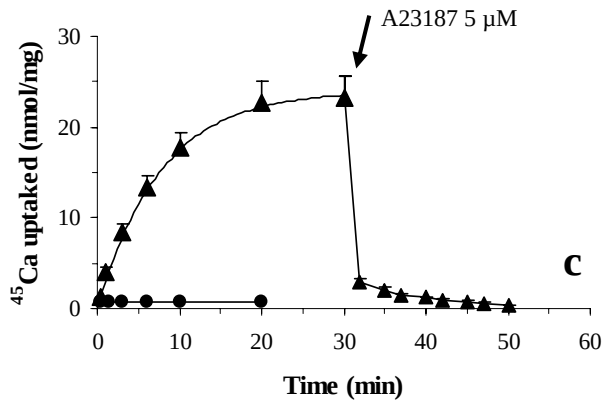
A23187 5 µM
45Ca uptaked (nmol/mg)
30
20
10
0
0
10
20
30
40
50
60
Time (min)
c

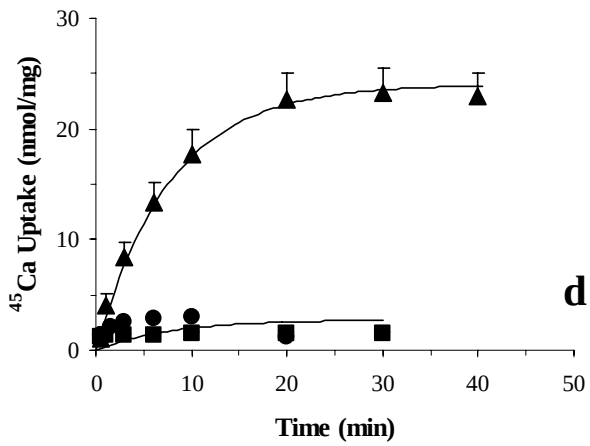
45Ca Uptake (nmol/mg)
30
20
10
0
0
10
20
30
40
50
Time (min)
d

Figure 1

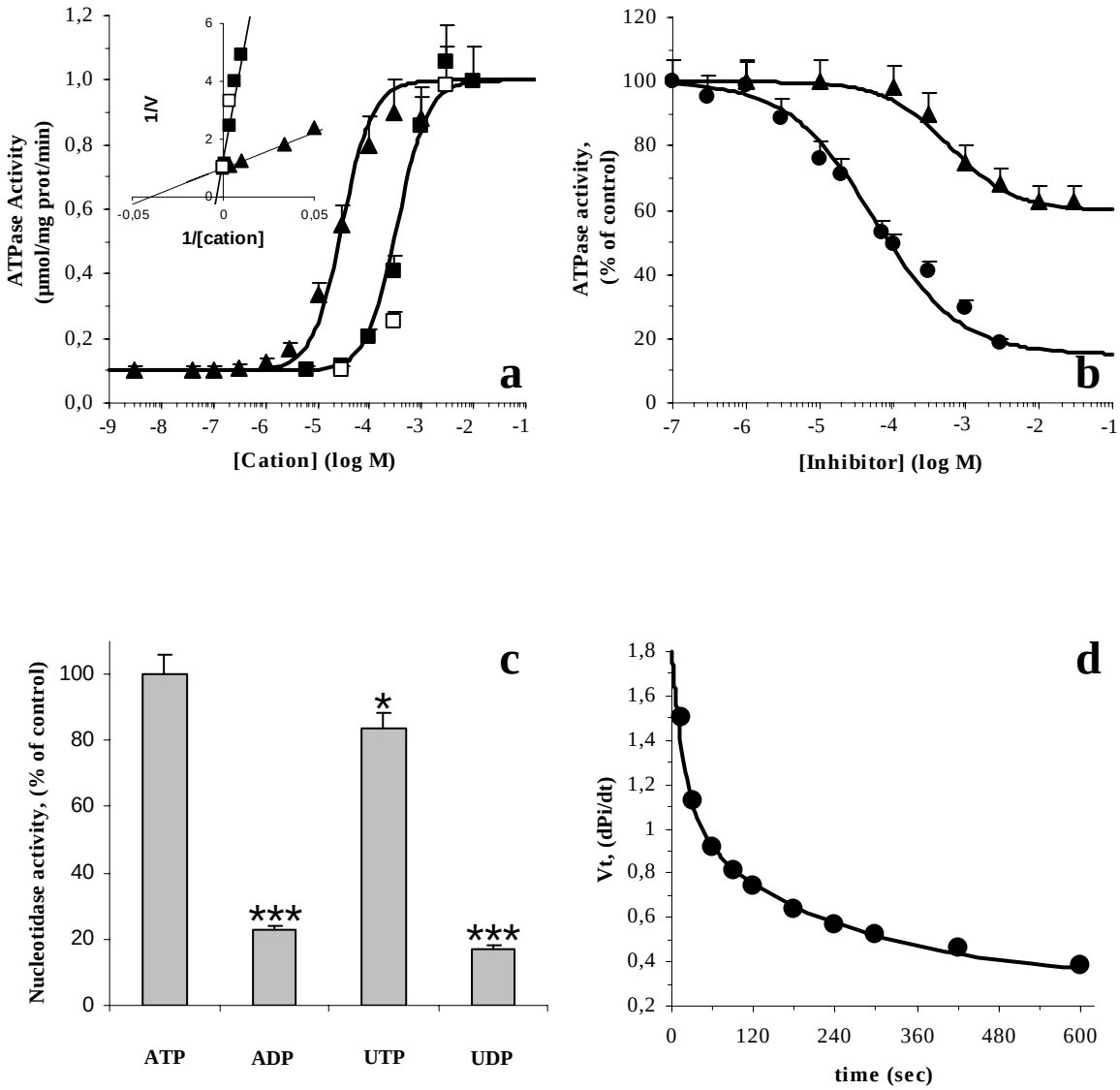
ATPase Activity (µmol/mg prot/min)
1,2
1,0
0,8
0,6
0,4
0,2
0,0
-9 -8 -7 -6 -5 -4 -3 -2 -1
[Cation] (log M)
a
1/V
6
4
2
0
-0,05 0 0,05
1/[cation]
ATPase activity, (% of control)
120
100
80
60
40
20
0
-7 -6 -5 -4 -3 -2 -1
[Inhibitor] (log M)
b
Nucleotidase activity, (% of control)
100
80
60
40
20
0
*
***
***
ATP
ADP
UTP
UDP
c
Vt, (dPi/dt)
1,8
1,6
1,4
1,2
1
0,8
0,6
0,4
0,2
0 120 240 360 480 600
time (sec)
d

Figure 2

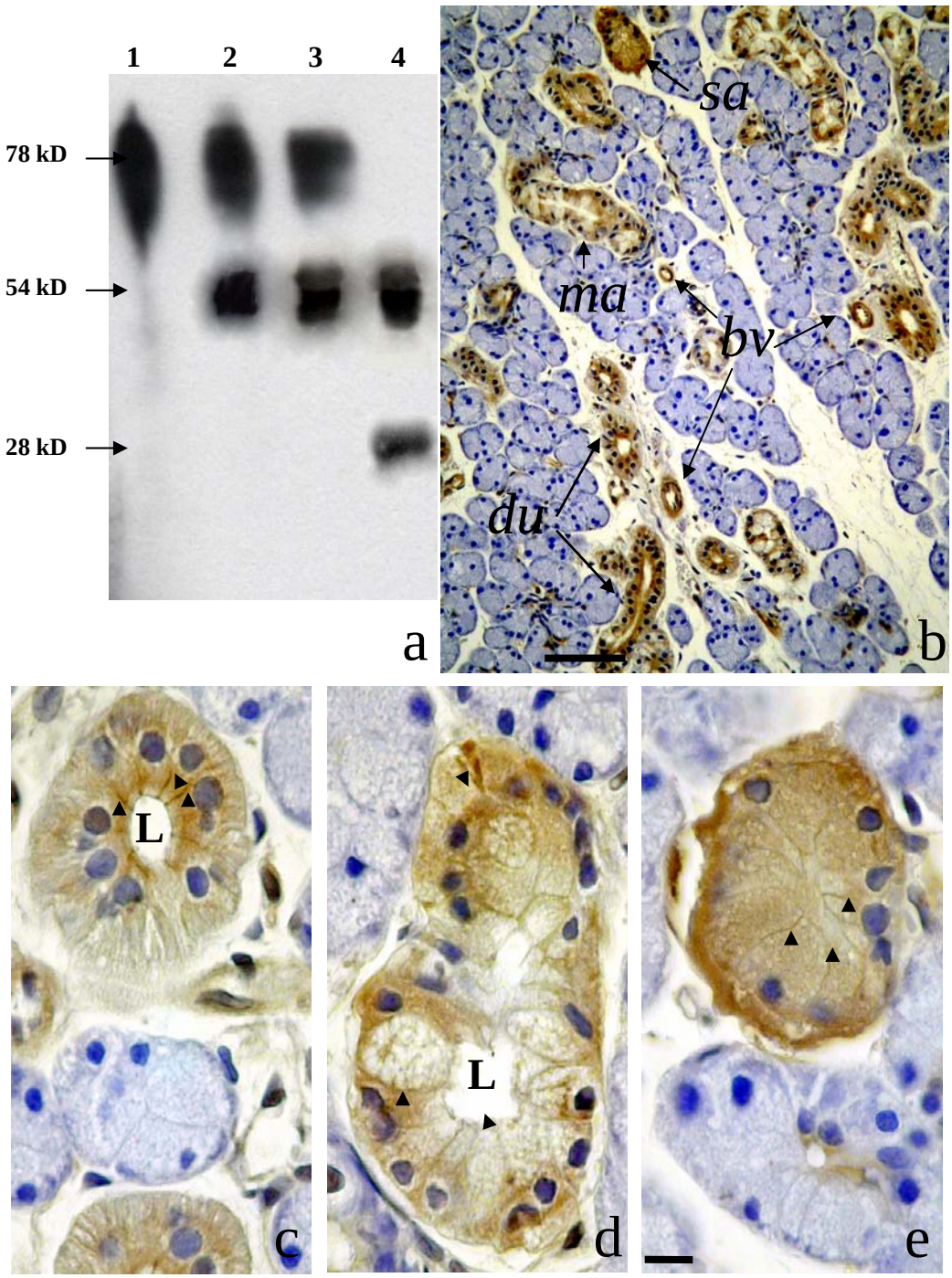

Figure 3

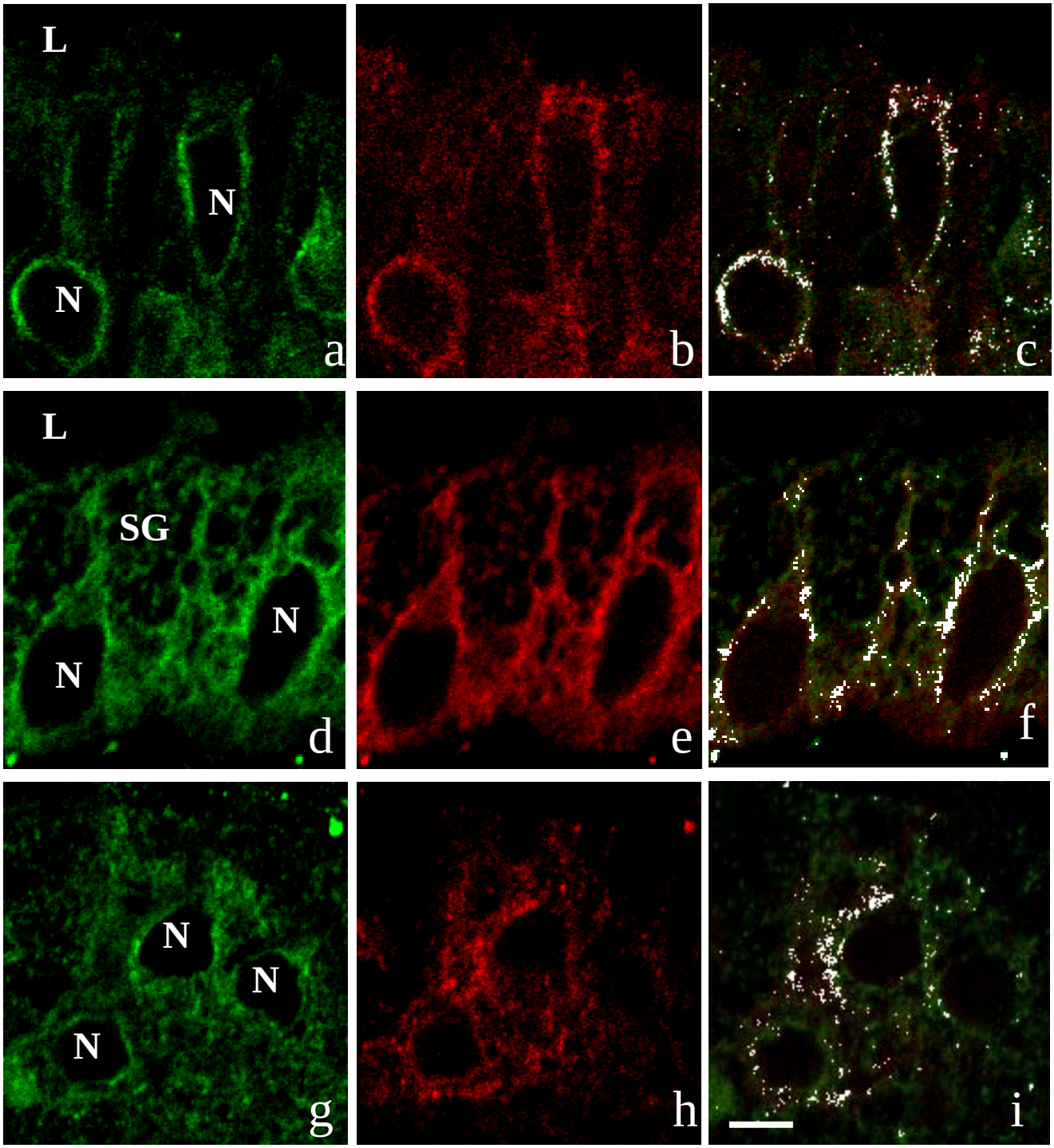

Figure 4